Integrating Deep Learning with eXplainable AI for Pixel-Based Analysis of Wildfire Severity with USGS FIREMON dNBRs in Turkey

Kavzoglu T. [1*] and Yilmaz E.O.[2]

[1]Prof. Dr., Department of Geomatics Engineering, Gebze Technical University, Turkey

[2] R.A., Department of Geomatics Engineering, Gebze Technical University, Turkey

*kavzoglu@gtu.edu.tr

Abstract: *Wildfires are a major natural catastrophe that disrupts the normal cycle of ecosystems, causing forests to be destroyed. Annually, a substantial amount of forest is devastated by wildfires around the globe. Reliable and accurate data about the burnt areas is crucial for assessing the amount of wildfire damage. Utilizing remote sensing and advance deep learning techniques provides significant advantages in enhancing the dependability and effectiveness of detecting burnt areas. This study examines the wildfires that occurred place during July 2023 around the Aegean region of Turkey. Within the scope of the study, classification was carried out with pixel-based Convolutional Neural Network (CNN) using Sentinel-2A imagery before and after the wildfires. Prior to classifying the severity of the fire, the dNBR values were computed and four distinct degrees of intensity were identified using the thresholds established in USGS FIREMON. Prior to generating wildfire severity classes for the training data set, dNBR values were computed and 4 distinct intensity levels were identified using thresholds specified in USGS FIREMON. Spectral indices (Burned Area Index-BAI and normalized difference vegetation index-NDVI) of pre- and post-fire Sentinel-2A images were calculated and included in the data set during classification. As a result of the burn severity classification, the overall accuracy was determined as 90.24% and the kappa coefficient was 86.98%. The results demonstrate that the model attained exceptional accuracy rates across all test data. Furthermore, the SHAP methodology, which is a globally explainable artificial intelligence method, was employed to comprehend the decision-making processes of the trained deep learning model and assess the efficacy of each feature inside the model. The SHAP findings revealed that both post-BAI and pre-BAI variables significantly influenced the decision-making process of the model. In conclusion, this study proves how effective deep learning technique with XAI method are in accurately assessing fire damage.*

Keywords: *CNN, wildfire, SHAP, USGS FIREMON, eXplainable AI*

Introduction

Forests, which cover around thirty percent of Earth's surface, provide biological and environmental equilibrium. In addition, they also regulate climate and increase genetic variety. These activities have several benefits, including conserving natural balance, sustaining the ecosystem, biodiversity, and sustainability (Kavzoğlu et al., 2021a). According to the FAO Global Forest Resources Assessment report by 2020, there were about 4.06 billion hectares or 31 percent of worldwide terrestrial region covered by forests.

However, over the past 30 years, 178 million hectares of forest have been lost (FAO, 2021). In 2023, The General Directorate of Forestry reported 23,363,071 hectares of forest in Turkey. Human-caused greenhouse gas emissions lead to climate change as deforestation increases. This circumstance reinforces the need of forest conservation and sustainable management in fighting climate change. Additionally, forests control atmospheric carbon and block climatic transformation in addition to saving biodiversity (Heinrich et al., 2021). Forest fires harm the physical, chemical, and biological equilibrium of ecosystem. Moreover, they could boost greenhouse gas emissions (Ribeiro-Kumara et al., 2020). Global climate change is worsening, creating a global climate crisis. Due to severe heat and dryness, the 6th Assessment Report of the Intergovernmental Panel on Climate Change predicts more forest fires globally (IPCC, 2021). The Mediterranean region is predicted to have more extended droughts and big forest fires, as well as lower precipitation and higher temperatures. The forest fires cause destruction particularly under hot, dry and windy conditions.

The General Directorate of Forestry Forestry Statistics for 2023 indicate that Turkey's forest lands increased from 20 million hectares in 1973 to 23.4 million hectares. Tüfekçioğlu and Tüfekçioğlu (2021) report that 58% of our country's forest resources are in fire-prone locations, particularly in Mediterranean and Aegean regions. In the past decade, annually, Turkey has experienced an average of 2388 forest fires which destroyed about 6665 hectares of its forests. The mega forest fires of 2021 caused significant damage and forest area losses (Kavzoğlu et al., 2021a; Tonbul, Colkesen, & Kavzoglu, 2022).

Monitoring, mapping and assessing burnt areas after wildfire is essential for sustainable forest fire management. Accurate and trustworthy fire information helps reduce fire causes, identify fire-prone regions, and development fire prevention tactics. In this regard, satellite images are key outcomes of remote sensing technology that assist in monitoring forest fires, mapping burnt areas, and assessing temporal changes. In attempt to collect precise information about forest fires happening in different geographic positions over time as well as across the forest fire investigations utilize remote sensing techniques.

In remote sensing with satellite images, mapping burned regions is a major key area of focus. Remote sensing tools are providing high resolution images more often as a result of technology advancement. Sentinel-2 satellite, introduced by the European Space Agency in 2015, has capable of taking high-resolution images every five days, for utilizing to monitor forest fires and other places. Various approaches, such as supervised classification, object-

based classification, spectral index analysis, and spectrum mixing, have been used to map post-fire situations (Kavzoğlu et al., 2021a; Tonbul et al., 2022; Filipponi, 2019). Vegetation burning leads to significant reductions in visible-near infrared reflectance (0.4-1.3 μm) through both combustion and loss of plant cover (Eva and Lambin, 1998). Spectra of burning and dense grass cover, sparse grass cover, and small shrubs with burning show gradual increase in reflectance in the 0.5-0.7 μm electromagnetic spectrum, while extensive vegetation spectra fluctuate. Due to this phenomenon, post-fire modifications on plant life are brought forth by burning and destruction. Evaporation decreases because charred plant absorbs more radiation than green vegetation. Increases in surface reflectance and temperature are detected in the shortwave infrared band (1.6-2.5 μm). The larger the spectral difference observed from land cover within a burnt area, the more extensive it had been damaged by fire (Brovkina et al., 2020). Fire intensity differences the spectral response of land cover (White et al., 1996). Post-fire modifications depend on plant community type, annual temperature trends during the vegetative season, and the time since the occurrence of a flame (Lentile et al., 2006). Normalized Difference Vegetation Index (NDVI), Burned Area Index (BAI), Normalized Burned Ratio (NBR), and Difference Normalized Burned Ratio (dNBR) can be used to detect burned areas by detecting broad spectral changes in vegetation. NBR and dNBR have gained the greatest popularity.

The research focuses on the forest fires that occurred place in Muğla province on 12 and 14 July 2023. It employs Sentinel-2 satellite images captured before the fire (11 July 2023) and after the fire (16 July 2023) to analyze the intensity of the fires using a deep learning method. Furthermore, pixel classification procedures were conducted using both the spectral bands and the vegetation and fire spectral indices. In addition, through explainable artificial intelligence methods applied to the models trained, it was studied how fire area determination occurred along with determining its severity.

Study Area and Dataset

This study analyzes the two consecutively took place forest fires in the Aegean Section of Turkey in 2023. For the research, Muğla province was selected as the study region due to the wildfires that occurred in Maya (region 2#) and Güvercinlik (region 1#) regions on 12 July and 14 July 2023 (Figure 1). Muğla province has a Mediterranean climate with hot-dry summers and mild-rainy winters. In general, Muğla province has a mountainous forested area covered with pine trees.

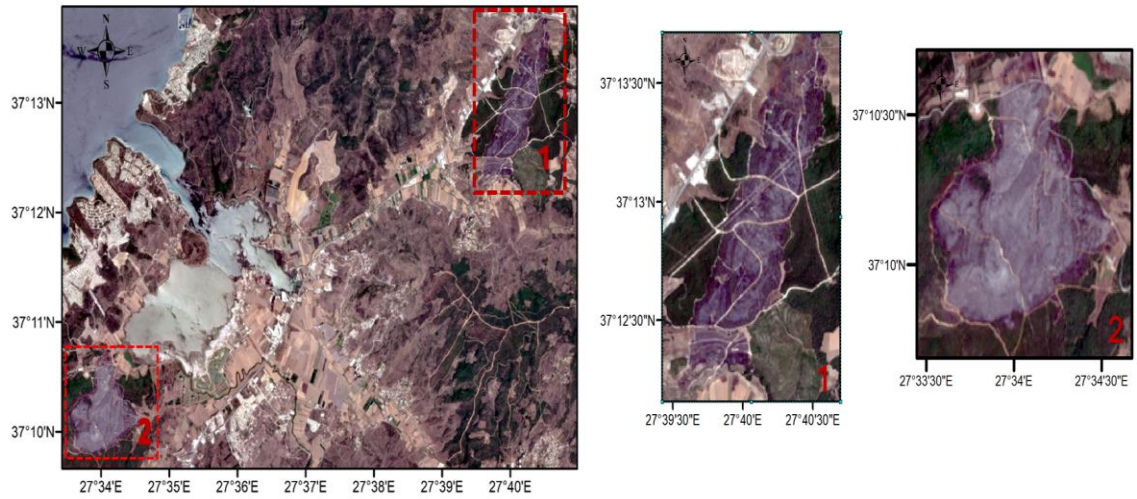

Figure 1: Study area with wildfire locations.

Two cloud-free Sentinel-2A satellite images from 11 July 2023 (pre-fire) and 16 July 2023 (post-fire) were utilized to assess forest conditions in the research region. The Sentinel-2A imagine has visible (Red-Green-Blue) and infrared bands with a spatial resolution of 10 m, red edge, infrared, and shortwave infrared bands with 20 m, and coastal aerosol, water vapor, and cirrus bands with 60 m. Copernicus Hub provided the satellite imagery of the study. Prior to processing images, all 60-m-resolution spectral bands were removed. The fire analysis data collection has just 10 m and 20 m spatial resolution bands. In a pre-processing step, the Gram-Schmidt method, a pan-sharpening technique, lowered all spectral bands with a spatial resolution of 20 m to 10 m.

Four different spectral indices were calculated for the deep learning-based classification stages and the determination of burning severity levels. These indices recognize the need for both burned and unburned regions. The formulas, abbreviations and reference sources of the indices used in the study are presented in Table 1.

Table 1: Spectral indices were used for detecting wildfire region.

Name	Abbr.	Formulas	References
Burnt Area Index	BAI	$\frac{1}{(0.1-\text{Bant}4)^2+(0.06-\text{Bant}8)^2}$	Chuvieco, Martín & Palacios, 2002
Normalized difference vegetation index	NDVI	$\frac{(\boldsymbol{Band8}-\boldsymbol{Band4})}{(\boldsymbol{Band8}+\boldsymbol{Band4})}$	Tucker, 1979
Normalize Burn Ratio	NBR	$\frac{(\boldsymbol{Band8}-\boldsymbol{Band12})}{(\boldsymbol{Band8}+\boldsymbol{Band12})}$	Key & Benson, 2005

Difference Normalized Burn Ratio	dNBR	$\boldsymbol{NBR_{pre-fire} - NBR_{post-fire}}$	Key & Benson, 2005; 2006

Within the scope of the study, the dNBR index was used for the sample identification of the burning severity level (unburned, low, moderate-low, moderate-high). Since there were very few samples at the high burning severity level, all of them were added to the moderate-high level.

Methodology

The CNN architectures, which are made up of several layers including convolutional, normalization, pooling, dense, and dropout layers, have gained significant popularity as deep learning models for extensive image applications (Yilmaz & Kavzoglu, 2021; Kavzoğlu & Yılmaz, 2022). CNNs use the characteristics of real information by employing four fundamental principles: local connections, weight sharing, pooling, and the incorporation of many layers (LeCun et al., 2015). By applying the exceptional characteristics of a dataset, it is possible to distinguish features without depending on human guided and complicated rules. CNNs consist of input, hidden, and output layers, which are important components regardless of their size. In the one-dimensional CNN model, the input layer consists of a one-dimensional matrix that contains the feature values. Convolutional layers consist of convolutional filters, and the weights are adjusted using the back-propagation approach. A series of trainable filters is used to convolve over the dataset generating several feature maps that fully cover the entire set. Convolutional processing efficiently recovers the most important characteristics of the dataset while minimizing the number of parameters and computer resources needed (Kavzoglu et al., 2021b).

Artificial intelligence (AI) systems that are currently in operation frequently possess an internal mechanism which is opaque systems (Temenos et al., 2023). These models have complex designs for outstanding performance. These designs may include hundreds of learnt parameters and a complicated mathematical representation (Speith, 2022). This reduces explainability. This may not essentially be an issue in decision-making that prioritizes performance more than logical thinking. Nevertheless, model explainability or interpretability are crucial, especially when taking significant decisions. For these issues, XAI offers numerous techniques to make opaque AI systems visible (Saeed and Omlin, 2023). XAI, which may be a rebirth of a new topic, has become a major study focus on several fields to improve the algorithm trust and responsibility. Furthermore, Shapley

Additive Explanation (SHAP), which is a XAI methods, interprets the outputs of machine/deep learning model (Lundberg and Lee, 2017). It operates by assigning each feature's prediction effect independently. SHAP values give an entire overview of a model predictions, including feature contributions and interactions. It clarifies how models predict. They are the total of the difference between the predicted and actual output for a sample, so they have a probabilistic explanation. The interpretation stage compares the contribution of different characteristics to a prediction and assesses explanation uncertainty.

Results and Discussion

Within the scope of the study, to produce fire severity maps of the study region, training and test data sets were created in a ratio of 70:30 with stratified random sampling technique. A total of 980 samples for the training data set and 420 samples for the test data set were collected within the boundaries of the study zone. Among the fires that occurred on two different dates within the study area, the forest fire that occurred in the northeastern part of the study area on 12 July 2023 was used for the training data set, while the forest fire that occurred in the southwestern part of the study area on 14 July 2023 was used as a test data set to evaluate the performance of deep learning algorithm.

The 1D-CNN model contains Conv1D, Batch Normalization, Dropout, Flatten, and Dense layers. The total number of parameters is 748,436, out of which 746,452 may be showed by training, while 1,984 parameters remain untrained. The initial layer consists of a Conv1D layer with 512 filters, which is then followed by Batch Normalization and Dropout layers. Following each Conv1D layer, this structure was replicated, with the number of filters decreasing gradually to 32. Ultimately, the data was compressed and the SoftMax activation function was chosen for the final output layer to classify the combustion levels into 512, 256, 128, 64, 32, 16, and 4 individual groups. This structure is designed to improve the ability of model to accurately categorize various degrees of combustion intensities. Dropout was used after each thick layer to mitigate the risk of overfitting.

The model parameters were obtained by an iterative process of trial and error. The Adamax algorithm was employed for optimization, and also the categorical cross entropy function was selected as the loss function. The training process was performed with 500 epochs and each epoch including a batch of 32 data. The parameters were selected to maximize the model's performance on the validation set. The observed performance increases, particularly after 500 epochs, suggest that these settings are successful in training the model.

Upon analyzing the learning curve of the 1D-CNN model during the training and validation stage, a notable increase in the performance of model is evident. Although the training loss (shown by the blue line) reduces fast, the validation loss (represented by the orange line) follows a similar pattern. However, after the 100th epoch, the validation loss stabilizes and continues with minor variations. The training accuracy, represented by the green line, and the validation accuracy, represented by the red line, exhibit a gradual rise with time and reach a plateau at around epoch 300. To summarize, the performance of model was satisfactory, but it might be further enhanced by implementing regularization techniques or data augmentation strategies to increase the accuracy of the validation process. No instances of overfitting were detected.

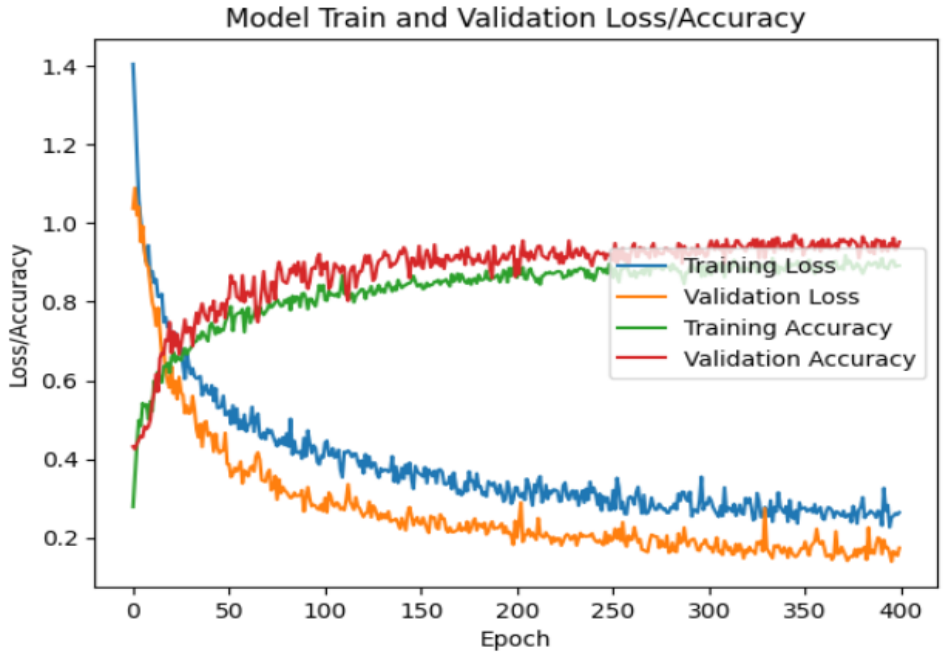

Figure 2: Learning curve for CNN model.

The thematic map displays the level of burn severity in a certain location after a forest fire, classified into four distinct levels (Figure 3). The colors on the map depict the spatial arrangement of burn severity. The green color signifies regions that remain unaffected by the wildfire, denoted as ‘Unburned’, whilst the yellow color represents areas of low severity. The orange color indicates areas with moderate-low severity, whereas the red color shows locations with the highest severity, specifically moderate-high severity areas damaged by the forest fire. It is worth mentioning that the red colors on the map are particularly

concentrated in the northeast and southwest regions, indicating the areas with the most intense forest fire activity. Furthermore, areas with different degrees of intensity are shown using yellow and orange colors. The map provides geographical coordinates and a distance scale, allowing for a clear understanding of the physical dimensions of the region in relation to the intensity information.

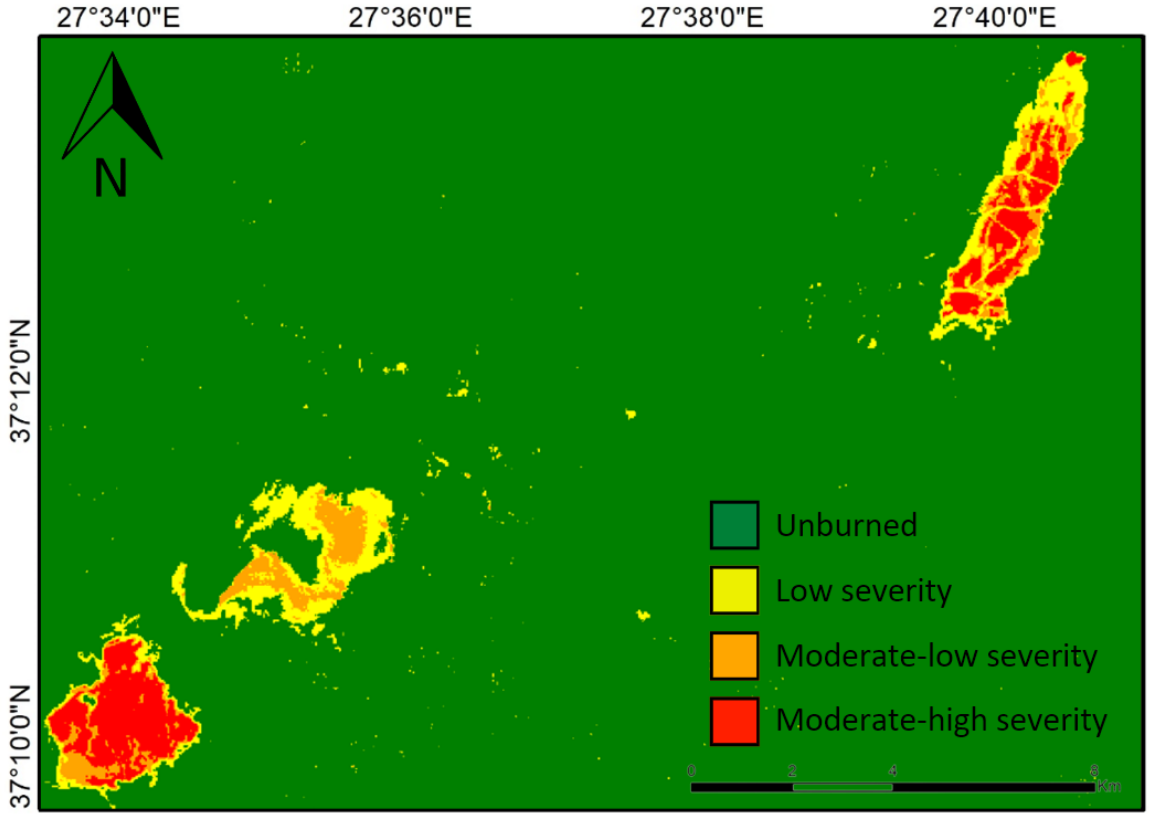

Figure 3: Burn severity thematic map produced using CNN model.

A pixel-based deep learning algorithm was used for the estimation of forest fire severity maps and levels. The accuracy of the model was measured by overall accuracy and Kappa coefficient, and the accuracy of the burn levels was measured by precision, sensitivity and F1 score metrics (Table 1). This study investigated the classification performance outcomes of the 1D-CNN model used to create fire severity maps. The model attained an accuracy of 85%, a recall of 95%, and an F1-score of 90% in the 'Unburned' class. The 'Low Severity Burn' class scored an accuracy of 96%, a recall of 84%, and an F1-score of 89%. The model obtained an accuracy of 94%, a recall of 87%, and an F1-score of 90% for the 'Moderate-Low Severity Burn' class. For the 'Moderate-High Severity Burn' class, the model achieved

an accuracy of 88%, a recall of 95%, and an F1-score of 91%. The overall accuracy of the model was determined to be 90.24%, while the Kappa coefficient was calculated to be 86.98%. The findings indicate that the model has a strong performance in accurately classifying fire severity maps.

Table 1: Accuracy assessment for forest fire severity map.

Burn Severity Class Names	Precision	Recall	F1-score
Unburned	0.85	0.95	0.90
Low severity	0.96	0.84	0.89
Moderate-low severity	0.94	0.87	0.90
Moderate-high severity	0.88	0.95	0.91
Overall Accuracy	0.9024		
Kappa Coefficient	0.8698		

Figure 4 illustrates the primary determinants of the output of model, as shown by the SHAP (SHapley Additive exPlanations) values. The SHAP chart illustrates the impact of inputs (spectral bands and indices) on the assessment of model of forest fire severity. The horizontal bars of graph depict the mean impact of each input on the model's output, with various colors indicating different fire severity classifications (Yellow: Medium-high severity burn, Red: Unburnt regions, Orange: Low severity burn, Green: Medium-low severity burn). The Post-BAI and Post-NDVI indices are the most influential inputs for the decision-making process. The 'Post-BAI' factor has a notable impact on all levels of wildfire severity. The Pre-BAI and Pre-NDVI indices play a crucial role and make a substantial contribution to the classification performance of the model. In addition, some spectral bands and indices, including Post-BAI and Pre-B8a, had a notable impact on the results of the model, particularly for regions that were unburned and burned with low intensity. The findings demonstrate that specific spectral bands and indices are crucial in determining the intensity of forest fires. Also, the SHAP values provide insight into the inputs that the model heavily depends on.

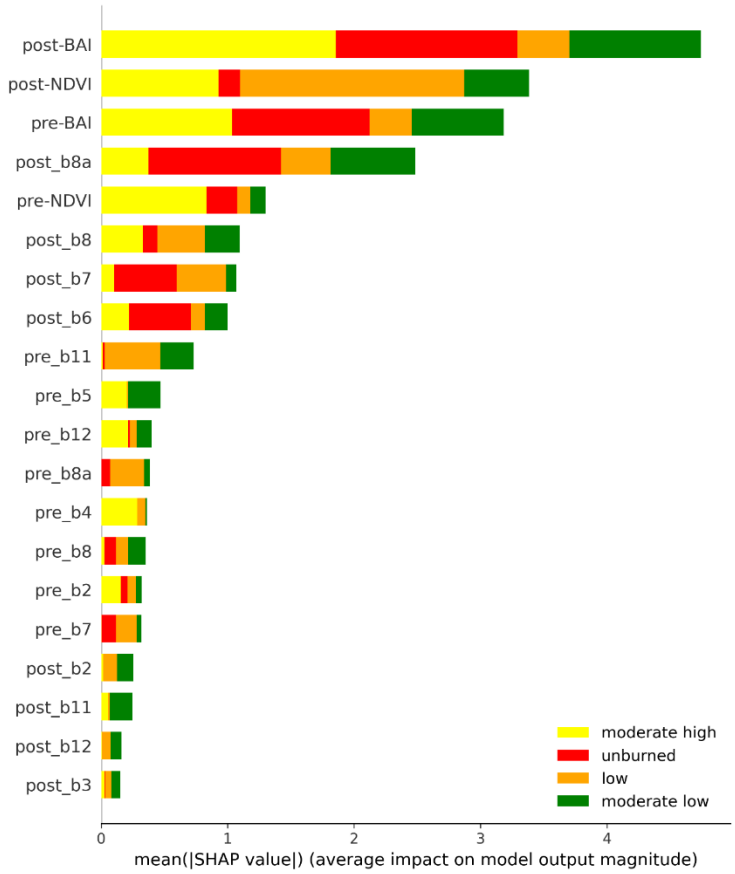

Figure 4: SHAP bar graph for the explainability of the decisions taken by the model in determining the burn levels

The SHAP beeswarm graphic illustrates the specific extent to which certain attributes contribute to the output of model. The x-axis represents the SHAP values, which indicate either a positive or negative impact. The characteristics of model are given on the vertical axis. The color gradient adjacent to the characteristics illustrates the range of values for each feature; colors of blue correspond to low values while colors of red correspond to high values. It clearly shows that the model output is significantly influenced by features such as post-NDVI and pre_b11. In addition, certain characteristics, such as post-NDVI, have a detrimental effect and others, such as post_b8a, have a beneficial effect. This research provides a comprehensive analysis of the bands and indices to which the model is more sensitive, as well as the specific attributes that have a greater impact on the output of model. This research is essential to gain a deeper understanding of the model's decision processes, particularly when dealing with complex remote sensing data.

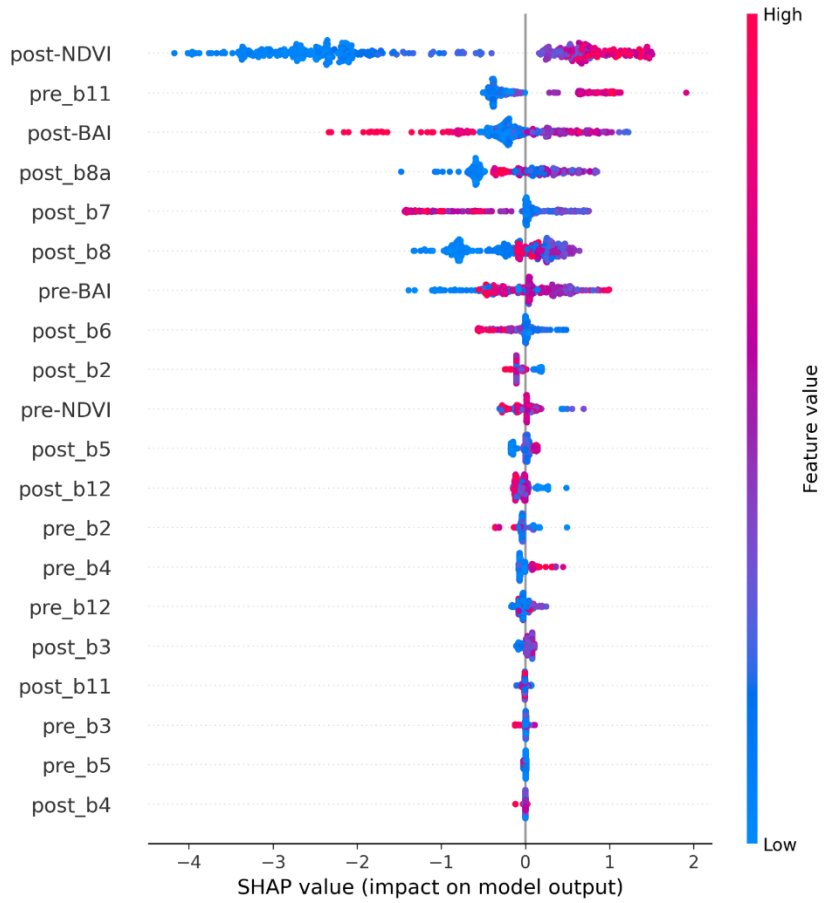

Figure 5: SHAP beeswarm graph to explain the decisions taken by the model in determining burn levels.

Conclusion and Recommendation

This work used a deep learning model to analyse the burn severity of post-fire sites and develop a thematic map. Burn severity was classified into four different categories: no burn, low severity, medium-low severity and medium-high severity. It was found that burn severity was concentrated in the north-eastern and south-western regions, resulting in significant fire impacts in these areas. It was recommended that natural regeneration processes should be monitored and that ecological treatments should be applied where necessary in low and medium burn severity areas. These findings provide important information for understanding post-fire ecosystem dynamics and guiding restoration initiatives. In addition, the use of XAI methods allowed us to gain a deeper understanding of the decision-making processes by studying the model. The SHAP studies identified the specific features and pixel groupings to which the model gave greater importance during the

prediction stage. The data collected from spectral bands in areas of high fire intensity had noticeable characteristics that resulted in a high level of prediction accuracy. Conversely, the model was found to have a higher degree of uncertainty in its conclusions and the accuracy of its predictions decreased in areas of low and moderate fire intensity. In addition, the SHAP results provided evidence for the effectiveness of the BAI and NVDI indices in detecting burned areas. To improve the performance of the model, it is recommended that the data be supplemented, and tests conducted on additional parameters, particularly in areas of low fire severity. The utilization of SHAP and other XAI methods develops the clarity of the model and contributions in decision making for ecosystem restoration and management.

References

Brovkina, O., Stojanović, M., Milanović, S., Latypov, I., Marković, N., & Cienciala, E. (2020). Monitoring of post-fire forest scars in Serbia based on satellite Sentinel-2 data. Geomatics, Natural Hazards and Risk, 11(1), 2315-2339. https://doi.org/10.1080/19475705.2020.1834002

Chuvieco, E., Martín, M. P., & Palacios, A. (2002). Assessment of different spectral indices in the red-near-infrared spectral domain for burned land discrimination. International Journal of Remote Sensing, 23(23), 5103-5110. https://doi.org/10.1080/01431160210153129

Eva, H., & Lambin, E. F. (1998). Remote sensing of biomass burning in tropical regions: Sampling issues and multisensor approach. Remote Sensing of Environment, 64(3), 292-315. https://doi.org/10.1016/S0034-4257(98)00004-4

FAO. (2021). Global forest resources assessment 2020: Main report. FAO. https://doi.org/10.4060/ca9825en

Filipponi, F. (2019). Exploitation of Sentinel-2 time series to map burned areas at the national level: A case study on the 2017 Italy wildfires. Remote Sensing, 11(6), 622. https://doi.org/10.3390/rs11060622

Heinrich, V. H., Dalagnol, R., Cassol, H. L., Rosan, T. M., de Almeida, C. T., Silva Junior, C. H., Campanharo, W. A., House, J. I., Sitch, S., Hales, T. C., & Adami, M. (2021). Large carbon sink potential of secondary forests in the Brazilian Amazon to mitigate climate change. Nature Communications, 12(1), 1785. https://doi.org/10.1038/s41467-021-22050-1

IPCC. (2021). Summary for policymakers. In V. Masson-Delmotte, P. Zhai, A. Pirani, S. L. Connors, C. Péan, S. Berger, N. Caud, Y. Chen, L. Goldfarb, M. I. Gomis, M. Huang, K. Leitzell, E. Lonnoy, J. B. R. Matthews, T. K. Maycock, T. Waterfield, O. Yelekçi, R. Yu, & B. Zhou (Eds.), Climate change 2021: The physical science basis. Contribution of Working Group I to the Sixth Assessment Report of the Intergovernmental Panel on Climate Change (pp. 1-41). Cambridge University Press. https://www.ipcc.ch/report/ar6/wg1/

Kavzoğlu, T., & Yılmaz, E. Ö. (2022). Analysis of patch and sample size effects for 2D-3D CNN models using multiplatform dataset: Hyperspectral image classification of ROSIS and Jilin-1 GP01 imagery. Turkish Journal of Electrical Engineering and Computer Sciences, 30(6), 2124-2144. https://doi.org/10.3906/elk-2203-88

Kavzoğlu, T., Çölkesen, İ., Tonbul, H., & Öztürk, M. Y. (2021a). Uzaktan algılama teknolojileri ile orman yangınlarının zamansal analizi: 2021 yılı Akdeniz ve Ege yangınları. In Orman yangınları: Sebepleri, etkileri, izlenmesi, alınması gereken önlemler ve rehabilitasyon faaliyetleri (pp. 219-252).

Türkiye Bilimler Akademisi.

Kavzoğlu, T., Teke, A., & Yılmaz, E. O. (2021b). Shared blocks-based ensemble deep learning for shallow landslide susceptibility mapping. Remote Sensing, 13(23), 4776. https://doi.org/10.3390/rs13234776

Key, C. H., & Benson, N. C. (2005). Landscape assessment: Ground measure of severity, the composite burn index, and remote sensing of severity, the normalized burn ratio. In FIREMON: Fire effects monitoring and inventory system (General Technical Report). U.S. Department of Agriculture, Forest Service, Rocky Mountain Research Station.

Key, C. H., & Benson, N. C. (2006). Landscape assessment (LA). In FIREMON: Fire effects monitoring and inventory system (General Technical Report). U.S. Department of Agriculture, Forest Service, Rocky Mountain Research Station.

LeCun, Y., Bengio, Y., & Hinton, G. (2015). Deep learning. Nature, 521(7553), 436-444. https://doi.org/10.1038/nature14539

Lentile, L. B., Holden, Z. A., Smith, A. M. S., Falkowski, M. J., Hudak, A. T., Morgan, P., & Benson, N. C. (2006). Remote sensing techniques to assess active fire characteristics and post-fire effects. International Journal of Wildland Fire, 15(3), 319-345. https://doi.org/10.1071/WF05097

Lundberg, S. M., & Lee, S. I. (2017). A unified approach to interpreting model predictions. In Advances in Neural Information Processing Systems (Vol. 30).

Ribeiro-Kumara, C., Köster, E., Aaltonen, H., & Köster, K. (2020). How do forest fires affect soil greenhouse gas emissions in upland boreal forests? A review. Environmental Research, 184, 109328. https://doi.org/10.1016/j.envres.2020.109328

Saeed, W., & Omlin, C. (2023). Explainable AI (XAI): A systematic meta-survey of current challenges and future opportunities. Knowledge-Based Systems, 263, 110273. https://doi.org/10.1016/j.knosys.2023.110273

Speith, T. (2022, June). A review of taxonomies of explainable artificial intelligence (XAI) methods. In Proceedings of the 2022 ACM Conference on Fairness, Accountability, and Transparency (pp. 2239-2250). https://doi.org/10.1145/3531146.3533198

Temenos, A., Temenos, N., Kaselimi, M., Doulamis, A., & Doulamis, N. (2023). Interpretable deep learning framework for land use and land cover classification in remote sensing using SHAP. IEEE Geoscience and Remote Sensing Letters, 20, 1-5. https://doi.org/10.1109/LGRS.2023.3245690

Tonbul, H., Çölkesen, İ., & Kavzoğlu, T. (2022). Pixel-and object-based ensemble learning for forest burn severity using USGS FIREMON and Mediterranean condition dNBRs in Aegean ecosystem (Turkey). Advances in Space Research, 69(10), 3609-3632. https://doi.org/10.1016/j.asr.2022.02.019

Tucker, C. J. (1979). Red and photographic infrared linear combinations for monitoring vegetation. Remote Sensing of Environment, 8(2), 127-150. https://doi.org/10.1016/0034-4257(79)90013-0

Tüfekçioğlu, A., & Tüfekçioğlu, M. (2021). Yangın sonrası orman toprağında meydana gelen değişim ve etkileşimler. In Orman yangınları: Sebepleri, etkileri, izlenmesi, alınması gereken önlemler ve rehabilitasyon faaliyetleri (pp. 89-110). Türkiye Bilimler Akademisi.

White, J. D., Ryan, K. C., Key, C. C., & Running, S. W. (1996). Remote sensing of forest fire severity and vegetation recovery. International Journal of Wildland Fire, 6, 125-136. https://doi.org/10.1071/WF9960125

Yılmaz, E. O., & Kavzoğlu, T. (2021). Analysis of the effect of training sample size on the performance of 2D CNN models. In Intercontinental Geoinformation Days (Vol. 2, pp. 241-244).